Weighted Robust Basis Function for Phase Unwrapping

Oscar Dalmau[1], Mariano Rivera[1] and Adonai Gonzalez[2]

[1] *Centro de Investigacion en Matematicas A. C., Jalisco S/N Col. Valenciana, 36240 Guanajuato, Guanajuato, Mexico.*

[2] *Centro de Investigaciones en Optica A. C., Loma del Bosque 115, 37150 Leon, Guanajuato, Mexico*

Abstract

This work presents a robust algorithm for phase unwrapping. The proposed algorithm is based on the expansion of the estimated phase through a linear combination of a set of Basis Functions. We present a novel weighted robust functional which is minimised using a two step strategy. This model allows us to reduce the influence of noise and to remove inconsistent pixels in the estimation of the unwrapped phase. The proposed model assumes that the phase is smooth. Under this assumption, experiments demonstrate that if the phase is corrupted by high levels of noise, our model presents a better performance than state of the art algorithms. For low levels of noise, the results are comparable.

Keywords: Phase unwrapping, robust estimation, radial basis functions

1. Introduction

The phase unwrapping process [1, 2, 3, 4, 5, 6] is an important stage for interferometric data processing, Synthetic Aperture Radar interferometry (SAR) [7, 8, 9, 10, 11, 12, 13, 14], Magnetic Resonance Imaging (MRI) [15], profilometry by fringe pattern projection [16], to mention just some applications. There are different approaches for phase unwrapping algorithms; some reviews on the topic are reported in [17, 18, 19, 20] and references therein.

According to Itoh [1], the first differences of the unknown unwrapped phase ϕ are related to the wrapped first differences of the wrapped phase ψ by

$$\phi(a) - \phi(b) = \mathcal{W}(\psi(a) - \psi(b)) + n, \tag{1}$$

where a and b are neighboring pixels, $\mathcal{W}$ is the wrapping operator, and n is a probable residual; see notation in Subsection 2.1. Then, the phase unwrapping process can be achieved by means of a least squares approach [21]; this discussed in more detail in Subsection 2.1. The main problem of least squares based formulations is that the residual n in (1) is not Gaussian, and as a consequence, the computed unwrapped phase may have large distortions [22]. In order to solve this problem, weighting techniques or robust formulations can be useful to achieve an accurate wrapped phase [20, 22, 23, 24].

On the other hand, a Radial Basis Functions (RBF) expansion for phase unwrapping was recently proposed in[25]. An advantage of the RBF based unwrapping method is the implicit filtering of the unwrapped phases. This method produces accurate wrapped phases when the noise level is relatively low. However, the results are severely deteriorated for high levels of noise. In this work, we propose a new model for phase unwrapping that also approximates the reconstructed phase through a linear combination of a set of functions. Similar to Ref. [25], we approximate the unwrapped phase using RBF, although our proposal has two main differences with respect to [25]: first, we based our model on a robust potential [24, 26], and second, we also introduced a novel weight to the robust functional, which allows us to control inconsistent pixels [22, 19]. These two modifications lead to a weighted robust functional for phase unwrapping which is less sensitive to noise and is also able to automatically remove inconsistent pixels in the parameter estimation process. The experimental results show a better performance of the proposed model over the least–squares–based RBF model for phase unwrapping [25] in the case of high levels of noise. When the noise level is low, the results of our approach are comparable to results achieved by state of the art methods, including the least–squares–based RBF model [25]. Since our method is based on RBF, it performs an implicit noise filtering, opposite to the robust unwrapping method recently reported in [4, 6, 20].

The structure of the paper is as follows. In Section 2 we present an overview of the phase unwrapping problem. Section 3 presents our proposal with a detailed description of the new model. Section 4 presents numerical experiments that compare the results achieved by our proposal with state of the art algorithms. Finally, in Section 5, we present our conclusions.

2. Brief review of phase unwrapping

In this section, we briefly explain the phase unwrapping problem and introduce the notation used in this work. Next, we briefly review the RBF approach for phase unwrapping [25].

2.1. Phase unwrapping description

Let $(x, y) \in \mathcal{L}$ be a pixel in the lattice $\mathcal{L} = \{(x, y)|x = 1, 2, \cdots, N_x; y = 1, 2, \cdots, N_y\}$, where N_x and N_y are the numbers of rows and columns of the image, respectively. Then, given the wrapped phase $\psi(x, y)$, the problem consists in computing the unwrapped phase $\phi(x, y)$; the phases are related through the *wrapping operator* $\mathcal{W}(\cdot) \in (-\pi, \pi]$ in the following way:

$$\psi(x, y) \quad = \mathcal{W}(\phi(x, y)) \stackrel{def}{=} \phi(x, y) + 2k(x, y)\pi, \tag{2}$$

$\forall (x, y) \in \mathcal{L}$, and $k(x, y) \in \mathbb{Z}$ is an integer field such that $\psi(x, y) \in (-\pi, \pi]$. In order to compute $\phi(x, y)$, one needs to invert the operator $\mathcal{W}$, which is equivalent to finding the integer field $k(\cdot, \cdot)$, which in turn is an ill-conditioned problem if no further information is added. Let us define the standard discrete derivatives and gradient as

$$\Delta_x \phi(x, y) = \phi(x + 1, y) - \phi(x, y), \tag{3a}$$

$$\Delta_y \phi(x, y) = \phi(x, y + 1) - \phi(x, y), \tag{3b}$$

$$\nabla \phi(x, y) = [\Delta_x \phi(x, y), \Delta_y \phi(x, y)]^T, \tag{3c}$$

and the wrapped discrete derivatives of $\psi(\cdot, \cdot)$ as follows:

$$\psi_x^\omega(x, y) \stackrel{def}{=} \mathcal{W}[\Delta_x \psi(x, y)], \tag{4a}$$

$$\psi_y^\omega(x, y) \stackrel{def}{=} \mathcal{W}[\Delta_y \psi(x, y)]. \tag{4b}$$

Assuming that $\exists (x, y)$, such that $|\nabla \phi(x, y)|_\infty > \pi$, one can estimate the unwrapped phase $\phi(x, y)$ using a standard least square formulation [22]. Since the least square procedure corresponds to the maximum likelihood estimation based on Gaussian noise (residuals), the classic least square algorithm for phase unwrapping is not reliable, since the wrapped phase is contaminated by impulsive noise produced by wrapping phase jumps larger than π [22].

2.2. Radial Basis Function for Phase Unwrapping

Ref. [25] presents an alternative to estimate the unwrapped phase $\phi(x, y)$ by means of linear combinations of RBF. They approximate the phase with a linear combination based on a single function (*i.e.*, RBF), and use the following expansion

$$\phi(x, y) = \sum_{i=1}^{N_i} \sum_{j=1}^{N_j} a_{ij} \phi_{ij}(x, y) = \boldsymbol{\phi}^T(x, y)\boldsymbol{a}, \tag{5}$$

where N_i, N_j correspond to the number of base functions in the 'x'- and 'y'-directions respectively, and the base functions $\phi_{ij}(x, y) = \phi_i(x)\phi_j(y)$ are equally spaced in the domain of the image. In particular, in [25] the authors use Gaussian functions:

$$\phi_k(z) \;=\; \exp\left(-\frac{(z-\mu_k)^2}{2\gamma_k^2}\right), \text{with} \quad z \in \{x, y\} \tag{6}$$

where μ_k, γ_k are the position and width of the Gaussian function, respectively; $\boldsymbol{\phi}(x, y)$ and $\boldsymbol{a}$ are the vectorisation[1] of the matrices $[\phi_{ij}(x, y)]$ and $[a_{ij}]$ respectively; *i.e.*,

$$\boldsymbol{\phi}(x, y) \;\stackrel{def}{=}\; vec\left([\phi_{ij}(x, y)]_{\substack{i=1,\cdots,N_i \\ j=1,\cdots,N_j}}\right). \tag{7}$$

If we define

$$\xi_k(z) \stackrel{def}{=} -\frac{z-\mu_k}{\gamma_k^2}, \tag{8}$$

and compute the gradient of $\phi(x, y)$ using the expansion (5), one obtains

$$\frac{\partial}{\partial x}\phi(x, y) = \sum_{i,j} a_{ij}\xi_i(x)\phi_{ij}(x, y) = \boldsymbol{\phi}_x^T(x, y)\boldsymbol{a}, \tag{9a}$$

$$\frac{\partial}{\partial y}\phi(x, y) = \sum_{i,j} a_{ij}\xi_j(y)\phi_{ij}(x, y) = \boldsymbol{\phi}_y^T(x, y)\boldsymbol{a}, \tag{9b}$$

[1]The vectorisation of a matrix is a linear transformation which converts the matrix into a column vector.

where $\boldsymbol{\phi}_x(x,y)$ and $\boldsymbol{\phi}_y(x,y)$ are the vectorisation of the matrices $[\xi_i(x)\phi_{ij}(x,y)]$ and $[\xi_j(y)\phi_{ij}(x,y)]$ respectively; *i.e.*,

$$\boldsymbol{\phi}_x(x,y) \stackrel{def}{=} vec\left([\xi_i(x)\phi_{ij}(x,y)]_{\substack{i=1,\cdots,N_i \\ j=1,\cdots,N_j}} \right), \tag{10a}$$

$$\boldsymbol{\phi}_y(x,y) \stackrel{def}{=} vec\left([\xi_j(y)\phi_{ij}(x,y)]_{\substack{i=1,\cdots,N_i \\ j=1,\cdots,N_j}} \right). \tag{10b}$$

We can write the least square cost function for phase unwrapping [19, 25] as follows

$$\begin{aligned} U(\boldsymbol{a}) \;\; = \sum_{(x,y)} \;\; & \left[\boldsymbol{\phi}_x^T(x,y)\boldsymbol{a} - \psi_x^{\omega}(x,y)\right]^2 \\ & + \left[\boldsymbol{\phi}_y^T(x,y)\boldsymbol{a} - \psi_y^{\omega}(x,y)\right]^2, \end{aligned} \tag{11}$$

or its corresponding matrix formulation

$$U(\boldsymbol{a}) \;\; = \;\; \|\boldsymbol{\Phi}_x\boldsymbol{a} - \boldsymbol{\psi}_x^{\omega}\|_2^2 + \|\boldsymbol{\Phi}_y\boldsymbol{a} - \boldsymbol{\psi}_y^{\omega}\|_2^2. \tag{12}$$

Then, the minimisation of the last function can easily be obtained with the following closed formula

$$\boldsymbol{a}^* \;\; = \;\; (\boldsymbol{\Phi}_x^T\boldsymbol{\Phi}_x + \boldsymbol{\Phi}_y^T\boldsymbol{\Phi}_y)^{-1}(\boldsymbol{\Phi}_x^T\boldsymbol{\psi}_x^{\omega} + \boldsymbol{\Phi}_y^T\boldsymbol{\psi}_y^{\omega}). \tag{13}$$

Thus, the estimation of the unwrapped phase is computed with

$$\hat{\phi}(x,y) \;\; = \;\; \boldsymbol{\phi}^T(x,y)\boldsymbol{a}^*, \; \forall (x,y) \in \mathcal{L}. \tag{14}$$

This approach is based on a least square formulation. The method yields a good phase reconstruction when the noise level is low and the phase is smooth, see Subsection 4.2; however, the results deteriorate when the noise level increases, principally producing a reduced dynamic range of the estimated phase. In the next subsection, we present a robust formulation that diminishes this problem.

3. Weighted Robust RBF for Phase Unwrapping

In order to solve the main problem of the RBF formulation for Phase Unwrapping, we present a weighted–robust formulation that tries to automatically remove the contribution of noise information in the estimation of

$\boldsymbol{a}$ and also takes into account the dynamic range problem of the RBF model. The new functional is

$$\begin{aligned} U(\boldsymbol{a}, s) \quad &= \sum_{(x,y)} \quad \upsilon^2(x,y)\Big(\rho\big(r_x(x,y)\big) + \rho\big(r_y(x,y)\big)\Big) \\ &\quad +\lambda(s-1)^2, \end{aligned} \tag{15}$$

where $\upsilon(x,y)$ is an inconsistency detector; *i.e.*, $\upsilon(x,y) = 1$ if (x,y) is an inconsistency site, and $\upsilon(x,y) = 0$ otherwise, $\rho(\cdot)$ is a robust function [26] and $r_x(x,y)$, $r_y(x,y)$ are residuals defined as follow:

$$r_x(x,y) = \boldsymbol{\phi}_x^T(x,y)\boldsymbol{a} - s\psi_x^{\omega}(x,y), \tag{16a}$$

$$r_y(x,y) = \boldsymbol{\phi}_y^T(x,y)\boldsymbol{a} - s\psi_y^{\omega}(x,y), \tag{16b}$$

where s is a scaling factor that allows correcting the dynamic range of the unwrapped phase, $\lambda > 0$ is a regularisation parameter, and finally, the last term of (15) promotes that the scaling factor be close to 1.

Inconsistent pixels as those where $\nabla \times \nabla\psi^{\omega}(x,y) \neq 0$ [19]. Thus, we suggest using the discrete version of the rotational operator:

$$\nabla \times \nabla\psi^{\omega}(x,y) = \sum_{i=1}^{4} \Delta_i, \tag{17a}$$

$$\Delta_1 = \mathcal{W}(\psi(x,y+1) - \psi(x,y)), \tag{17b}$$

$$\Delta_2 = \mathcal{W}(\psi(x+1,y+1) - \psi(x,y+1)), \tag{17c}$$

$$\Delta_3 = \mathcal{W}(\psi(x+1,y) - \psi(x+1,y+1)), \tag{17d}$$

$$\Delta_4 = \mathcal{W}(\psi(x,y) - \psi(x+1,y)). \tag{17e}$$

In order to detect inconsistent pixels, we suggest using the following weighting function:

$$\upsilon(x,y) \quad = \quad \frac{\alpha}{\alpha + (\nabla \times \nabla\psi^{\omega}(x,y))^2}, \tag{18}$$

where $\alpha > 0$ is a small value; *i.e.*, $\alpha = 0.01$. If $\upsilon(x,y) \approx 0$, it means that the site (x,y) is an inconsistent pixel, and it will not be taken into account in the parameter estimation; otherwise, if $\upsilon(x,y) \approx 1$, the site (x,y) is not inconsistent and is considered in the parameter estimation. As robust function ρ, we use the following differentiable approximation of the L_1–norm,

$$\rho(x) \quad = \quad \beta(x^2 + \beta^2)^{\frac{1}{2}}, \tag{19}$$

where $\beta > 0$ is related to the noise level detection. Then, according to [26], the weight function is

$$\nu^2(x) \stackrel{def}{=} \frac{\rho\prime(x)}{2x} = \beta(x^2+\beta^2)^{-\frac{1}{2}}. \tag{20}$$

Observe that the optimisation problem

$$\boldsymbol{a}^*, s^* = \underset{\boldsymbol{a},s}{\operatorname{argmin}}\, U(\boldsymbol{a}, s), \tag{21}$$

is non-linear. In order to solve the previous optimisation problem, we use a two-step algorithm. The algorithm first computes $\boldsymbol{a}$, and then the scaling factor s; *i.e.*,

1. $\boldsymbol{a}^* = \arg\min_{\boldsymbol{a}} U(\boldsymbol{a}, s)$, keeping fixed $s = 1$.
2. $s^* = \arg\min_s U(\boldsymbol{a}, s)$, keeping fixed $\boldsymbol{a} = \boldsymbol{a}^*$.

The final estimation of the unwrapped phase, $\hat{\phi}$, is computed with

$$\hat{\phi}(x,y) = \frac{1}{s^*}\boldsymbol{\phi}^T(x,y)\boldsymbol{a}^*,\ \forall (x,y) \in \mathcal{L}, \tag{22}$$

where $\boldsymbol{\phi}(x,y)$ is obtained using the Eq. (7). We note that both optimisation problems can be solved using an iterative process in which parameters are given by closed-form updating formulas. In order to see this, let us define the following weight functions:

$$\omega_x(x,y) \stackrel{def}{=} \upsilon(x,y)\nu(r_x(x,y)), \tag{23a}$$

$$\omega_y(x,y) \stackrel{def}{=} \upsilon(x,y)\nu(r_y(x,y)). \tag{23b}$$

An alternative to minimise efficiently $U(\boldsymbol{a}, s)$ is to take advantage of the matrix formulation:

$$\begin{aligned}\tilde{U}(\boldsymbol{a}, s) &= \|\tilde{\boldsymbol{\Phi}}_x\boldsymbol{a} - s\tilde{\boldsymbol{\psi}}_x^{\omega}\|_2^2 + \|\tilde{\boldsymbol{\Phi}}_y\boldsymbol{a} - s\tilde{\boldsymbol{\psi}}_y^{\omega}\|_2^2 \\ &\quad +\lambda(s-1)^2,\end{aligned} \tag{24}$$

where

$$\tilde{\boldsymbol{\phi}}_x(x,y) = \omega_x(x,y)\boldsymbol{\phi}_x(x,y), \tag{25a}$$

$$\tilde{\boldsymbol{\phi}}_y(x,y) = \omega_y(x,y)\boldsymbol{\phi}_y(x,y), \tag{25b}$$

$$\tilde{\psi}_x^{\omega}(x,y) = \omega_x(x,y)\psi_x^{\omega}(x,y), \tag{25c}$$

$$\tilde{\psi}_y^{\omega}(x,y) = \omega_y(x,y)\psi_y^{\omega}(x,y). \tag{25d}$$

Algorithm 1 WRRU Algorithm for Phase Unwrapping

Given: $\boldsymbol{\phi}_x, \boldsymbol{\phi}_y$, Eqs. (10a)-(10b), $\psi_x^{\omega}, \psi_y^{\omega}$, Eqs. (23a)-(23b), $\omega_x(x,y) = 1, \omega_y(x,y) = 1, \forall (x,y) \in \mathcal{L}$ and parameters (μ_i, μ_j), (γ_i, γ_j), $i = 1, \cdots, N_i$, $j = 1, \cdots, N_j$

{ **Step 1**: Compute $\boldsymbol{a}^*$ }

for $t = 1, 2, \cdots$ **do**

Obtain the matrices $\tilde{\boldsymbol{\Phi}}_x, \tilde{\boldsymbol{\Phi}}_y$, using Eqs. (25a)-(25b)

Compute vectors $\tilde{\boldsymbol{\psi}}_x^{\omega}, \tilde{\boldsymbol{\psi}}_y^{\omega}$, using Eqs. (25c)-(25d)

Compute $\boldsymbol{a}$ using Eq. (26)

Update ω_x, ω_y with $s = 1$ using Eqs. (23a)-(23b)

end for

{ **Step 2**: Compute s^* }

$\boldsymbol{a} = \boldsymbol{a}^*$ where $\boldsymbol{a}^*$ is the solution of the previous step

for $t = 1, 2, \cdots$ **do**

Obtain the matrices $\tilde{\boldsymbol{\Phi}}_x, \tilde{\boldsymbol{\Phi}}_y$, using Eqs. (25a)-(25b)

Compute vectors $\tilde{\boldsymbol{\psi}}_x^{\omega}, \tilde{\boldsymbol{\psi}}_y^{\omega}$, using Eqs. (25c)-(25d)

Compute s using Eq. (27)

Update ω_x, ω_y using Eqs. (23a)-(23b)

end for

Compute $\hat{\phi}$ with Eq. (22)

The solution of the first problem is obtained by repeating until convergence the following updating formula, with $s = 1$,

$$\boldsymbol{a} = s(\tilde{\boldsymbol{\Phi}}_x^T \tilde{\boldsymbol{\Phi}}_x + \tilde{\boldsymbol{\Phi}}_y^T \tilde{\boldsymbol{\Phi}}_y)^{-1}(\tilde{\boldsymbol{\Phi}}_x^T \tilde{\boldsymbol{\psi}}_x^{\omega} + \tilde{\boldsymbol{\Phi}}_y^T \tilde{\boldsymbol{\psi}}_y^{\omega}). \quad (26)$$

Note that $\tilde{\boldsymbol{\Phi}}_x$, $\tilde{\boldsymbol{\Phi}}_y$, $\tilde{\boldsymbol{\psi}}_{\omega}^{y}$ and $\tilde{\boldsymbol{\psi}}_{\omega}^{x}$ change at each iteration due to the weights ω_x and ω_y depend on the value of $\boldsymbol{a}$ in the previous iteration. Here, we denote the solution to Eq. (26) by $\boldsymbol{a}^*$. Similarly, the solution for the second problem is obtained by repeating until convergence the following updating formula:

$$s = \frac{[(\tilde{\boldsymbol{\psi}}_x^{\omega})^T \tilde{\boldsymbol{\Phi}}_x + (\tilde{\boldsymbol{\psi}}_y^{\omega})^T \tilde{\boldsymbol{\Phi}}_y]\boldsymbol{a}^* + \lambda}{\|\tilde{\boldsymbol{\psi}}_x^{\omega}\|_2^2 + \|\tilde{\boldsymbol{\psi}}_y^{\omega}\|_2^2 + \lambda}. \quad (27)$$

A pseudo code of the algorithm for computing $\boldsymbol{a}^*$, s^* and estimating $\hat{\phi}$ with Eq. (22) is presented as Algorithm 1.

4. Experiments

In this section, we present a numerical comparison of our proposal with 5 algorithms for phase unwrapping. In the comparison, we include the following algorithms: RBF for phase unwrapping (RBFU) [25], Accumulation of residual maps (ARM) [20], Phase unwrapping via graph cuts (PUMA) [4], Quality Guided Phase Unwrapping (QGPU) [6] and Costantini's [3]. We also present two variants of the proposed algorithm: Robust RBF without weight function for inconsistency detection (RRU), *i.e.*, $\upsilon(x, y) = 1$, and the Weighted Robust RBF with the weight function for inconsistency detection (WRRU), *i.e.*, $\upsilon(x, y)$ computed with Eq. (18).

4.1. Datasets and parameter description

In the experiments, we use the following wrapped phases (test functions)

$$\psi_\ell(x, y) = \mathcal{W}(f_\ell(x, y) + \eta),\ \ell = 1, 2, 3, 4; \quad (28)$$

for $x \in \{1, 2, \cdots, N_x\}$, $y \in \{1, 2, \cdots, N_y\}$ and $\eta \stackrel{def}{=} \eta(x, y) \sim \mathcal{N}(0, \sigma)$ is normal white noise with standard deviation $\sigma \in [0, 1]$. For illustration purposes, in Fig. 1, we show the wrapped phases obtained from Eq.(28) without noise;

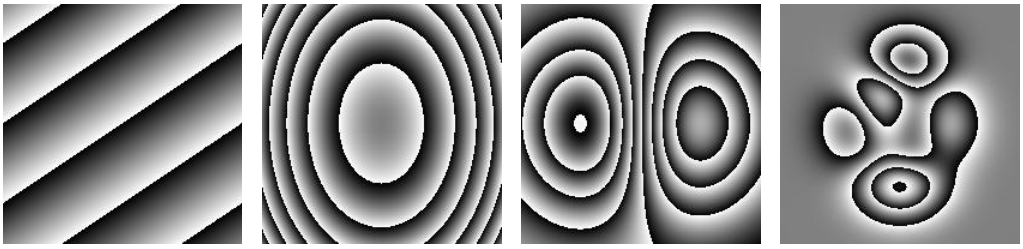

(a) ψ_1 (b) ψ_2 (c) ψ_3 (d) ψ_4

Figure 1: Test wrapped phases used in the experiments, obtained from Eq. (28) with $\eta = 0$.

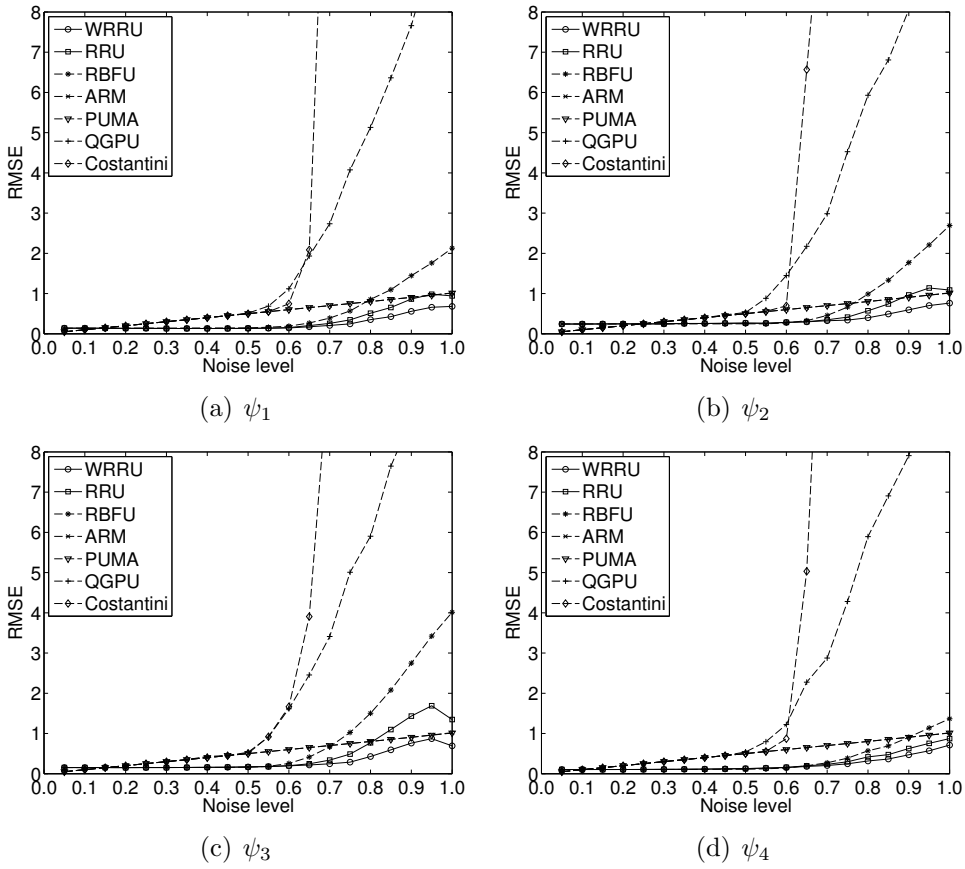

(a) ψ_1 (b) ψ_2

(c) ψ_3 (d) ψ_4

Figure 2: Average of the Root Mean Square Error between the estimated unwrapped phases and the original phases (without noise), see Fig. 1. The tested algorithms are WRRU, RRU, RBFU, ARM, PUMA, QGPU and Costantini's.

i.e., $\eta = 0$. The wrapped phases in Eq. (28) are generated from the following functions (or phases):

$$f_1(x,y) = \frac{4\pi}{N_x}x + \frac{6\pi}{N_y}y, \tag{29a}$$

$$f_2(x,y) = 32\pi\, x_c^2 + 16\pi\, y_c^2, \tag{29b}$$

$$f_3(x,y) = 160 x_c \exp\left(-8(x_c^2 + y_c^2)\right) + 2, \tag{29c}$$

$$f_4(x,y) = 2\,\text{peaks}(x,y), \tag{29d}$$

where

$$x_c = \frac{x}{N_x} - \frac{1}{2} \text{ and } y_c = \frac{y}{N_y} - \frac{1}{2},$$

and peaks$(\cdot,\cdot)$ is a built-in Matlab function.

In the experiments, we fix $N_x = N_y = 200$, and as noise standard deviation we use the following discretisation: $\sigma_n = \frac{n}{N}$, $n = 1, 2, \cdots, N$ with $N = 20$. For the parameter λ we use $\lambda_n = 10^6(10 - 9.5\sigma_n)$. The basis functions $\phi_{ij}(x,y)$ are equally spaced in the domain of the image, and in the experiments, we use RBFs with Gaussian profiles. The number of basis functions that were used is 144; *i.e.*, 12 in each direction $N_i = N_j = 12$, with $\gamma_i = \gamma_j = 1.3N_x/N_i$.

4.2. Numerical experiments

In this section, we present two numerical experiments. The first experiment evaluates the performance of the proposed algorithm for different levels of noise, and also includes a quantitative comparison with respect to RBFU, ARM, PUMA, QGPU and Costantini's algorithms. The experiment uses the test phases, Eq. (28), with different levels of noise: $\sigma_n = \frac{n}{N}$, $n = 1, 2, \cdots, N$ with $N = 20$. For each level of noise, we run 30 experiments and compute the Root Mean Square Error (RMSE) between the reconstructed phase $\hat{\phi}$ and the original phase f without noise, Eqs. (29a)-(29d):

$$RMSE(\hat{\phi}, f) = \sqrt{\frac{1}{N_x N_y}\sum_{x,y}\left(\hat{\phi}(x,y) - f(x,y)\right)^2}. \tag{30}$$

We report the average of the RMSE over the 30 experiments using WRRU, RRU, RBFU, ARM, PUMA, QGPU and Costantini's algorithms, see results in Fig. 2. We note that, when the noise standard deviation is less than 0.5, the performance of RBFU, RRU and WRRU algorithms is practically the

same. However, when the noise level increases, $\sigma_n \in (0.5, 1]$, it is clear that the new proposals have a better performance compared to the remainder algorithms. In particular, the version that controls the inconsistent pixels, WRRU, presents the best results.

In Fig. 3, we present the second numerical experiment using $\sigma_n = 1$. Table 1 summarises the corresponding numerical result. Similarly to the first experiment, the proposed algorithm WRRU presents the best performance.

Table 1: Root Mean Square Error of the WRRU, RRU, RBFU, ARM, PUMA, QGPU and Costantini's algorithms using the images in the first column of Fig. 3.

	Image Panel (a)	Image Panel (b)	Image Panel (c)	Image Panel (d)
WRRU	**0.6281**	**0.7766**	**0.6750**	**0.7770**
RRU	0.8411	1.3097	1.4947	1.1254
RBFU	1.9964	2.9373	4.1766	1.6571
ARM	1.0184	1.0167	1.0120	1.0133
PUMA	0.9995	1.0104	1.0129	1.0148
QGPU ($\times 10$)	1.0210	0.9849	1.0904	0.9147
Costantini ($\times 10^3$)	0.4456	0.2276	0.0612	1.5889

4.3. Experiment on weighting functions

This subsection illustrates the role of the weighting functions (23a)-(23b) for the WRRU algorithm. We include an experiment by varying the noise level parameter: $\sigma_n = \frac{n}{10}$, $n = 7, 8, 9, 10$. Fig 4 depicts the inconsistency detection process. This figure shows the weighting maps $\omega_x(x, y) + \omega_y(x, y)$ obtained by the unwrapping of the phases ψ_4 for each σ_n value. We note that the *weighting map* is capable of detecting inconsistent pixels (pixels in black in Fig. 4). The detection of inconsistent pixels is more notable when the values of σ_n are higher. We also note that WRRU is robust to noise. The noisy detected pixels correspond to gray level pixels; *i.e.*, intensity values in $(0, 1)$, in the weighting maps of Fig. 4.

4.4. Experiment with real data

Now, we present a qualitative (visual) comparison of the unwrapping methods using real data (the ground true is unknown), see Fig. 5. Panel (a) shows a real interferogram, and Panel (b) shows the corresponding wrapped phase. In order to fairly compare the analysed algorithms, we apply a DC

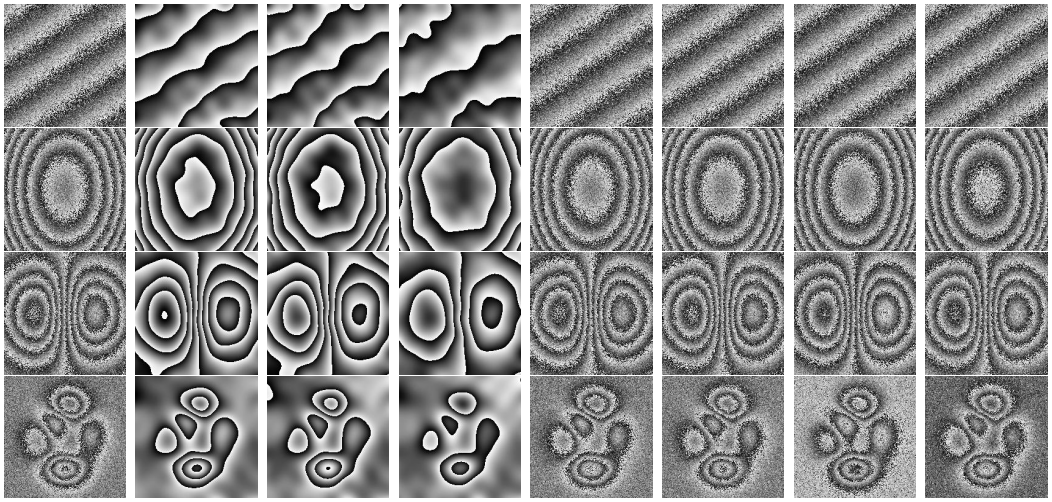

Figure 3: From left to right: wrapped phases obtained from Eqs. (28) with $\sigma = 1$ and rewrapping of the unwrapped phases computed with WRRU, RRU, RBFU, ARM, PUMA, QGPU and Costantini's algorithms, respectively.

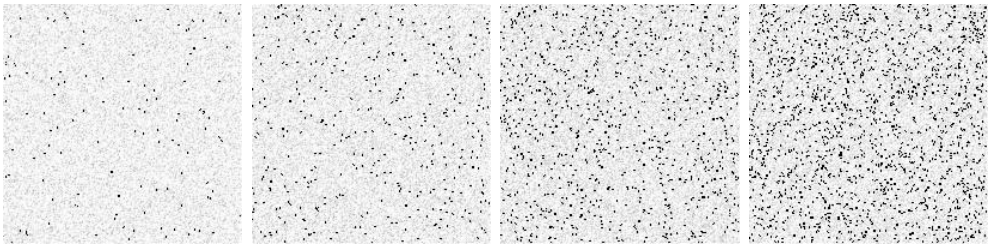

Figure 4: Illustration of the noise/inconsistencies detection. From left to right, maps of $\omega_x(x,y)+\omega_y(x,y)$ for wrapped phases obtained from ψ_4 using $\sigma_n = n/10$ for $n = 7, 8, 9, 10$.

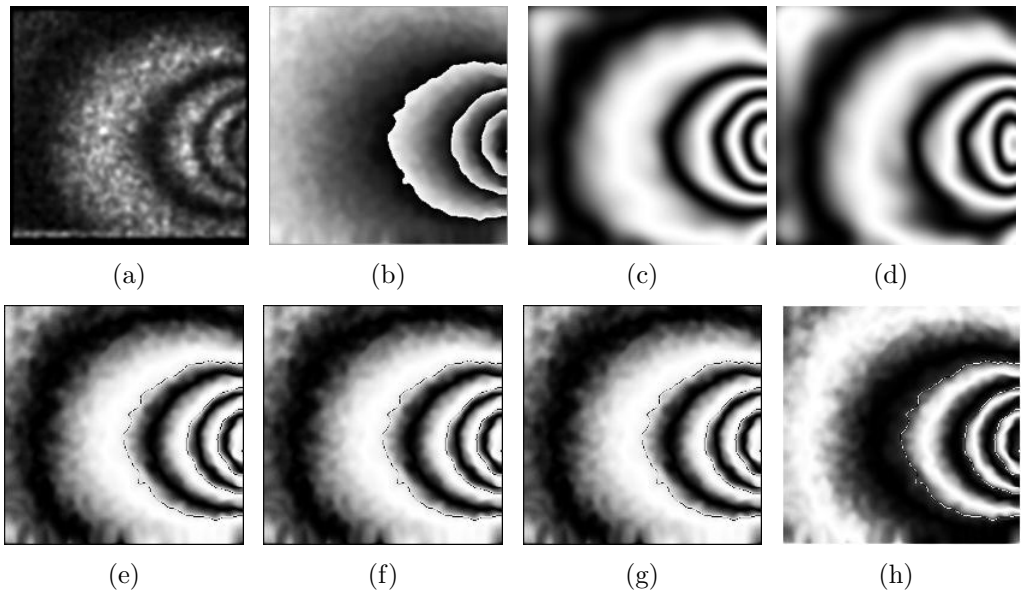

Figure 5: Fringe patterns from unwrapped phase obtained using different algorithms. (a) Original fringe pattern, (b) Original wrapped phase, (c) WRRU, (d) RBFU, (e) ARM, (f) PUMA, (g) QGPU and (h) Costantini's.

correction to the phase estimated by the algorithms. For this purpose, we solve the following optimisation problem

$$E(\hat{\phi}, p; d) = \sqrt{\frac{1}{N_x N_y} \sum_{x,y} \Big(p(x,y) - \cos(\hat{\phi}(x,y) + d)\Big)^2}, \tag{31}$$

$$d^* = \arg\min_d E(\hat{\phi}, p; d), \tag{32}$$

where p represents the original fringe pattern, see Panel (a) from Fig. 5, $\hat{\phi}$ represents the estimated phase, d^* is the optimum step correction, and $\hat{\phi}(x,y) + d^*$ is the estimated final phase. The estimated fringe patterns, $\cos(\hat{\phi}(x,y) + d^*)$, obtained by different algorithms are shown in Fig. 5. We observe that the unwrapped phases using RBF based methods are filtered; this can be noted in the cosine of the unwrapped phases.

5. Conclusions

In this work, we present two robust phase unwrapping algorithms. Our algorithms compute the phase by means of a linear combination of a set

of Basis Functions that simultaneously achieve a filtered unwrapped phase. The proposed algorithms are very general, and they can work using any set of Basis Functions. In particular, for the experiments presented in this work, we used Radial Basis Functions with Gaussian profile. The new framework is presented as a weighted robust functional that allows reducing the influence of noise data and inconsistency pixels in the parameter estimation. An advantage of the proposed algorithms is the implicit filtering of the unwrapped phases. Additionally, our proposal takes into account the dynamic range problem of the RBF for phase unwrapping. According to our experiments, the proposed model yields a better performance for high-noise levels and smooth phases. Moreover, it is clear that the weighted proposed algorithms overcome the unweighted RBF version.

Acknowledgments

We thank Dr. Amalia Martinez from the Laboratory of Optical and Mechanics Testing (CIO, Mexico) for supplying the real interferogram; we also thank the support from Mexico's "Consejo Nacional de Ciencia y Tecnologia" (CONACYT) (research grants: 131369 and 169178-F).

6. References

[1] K. Itoh, Analysis of the phase unwrapping algorithm, Appl. Opt. 21 (14) (1982) 2470–2470.

[2] T. J. Flynn, Two-dimensional phase unwrapping with minimum weighted discontinuity, J. Opt. Soc. Am. A 14 (10) (1997) 2692–2701.

[3] M. Costantini, A novel phase unwrapping method based on network programming, Geoscience and Remote Sensing, IEEE Transactions on 36 (3) (1998) 813–821.

[4] J. Bioucas-Dias, G. Valadao, Phase unwrapping via graph cuts, Image Processing, IEEE Transactions on 16 (3) (2007) 698–709.

[5] Q. Kemao, W. Gao, H. Wang, Windowed Fourier-filtered and quality-guided phase-unwrapping algorithm, Appl. Opt. 47 (29) (2008) 5420–5428.

[6] M. Zhao, L. Huang, Q. Zhang, X. Su, A. Asundi, Q. Kemao, Quality-guided phase unwrapping technique: comparison of quality maps and guiding strategies, Appl. Opt. 50 (33) (2011) 6214–6224.

[7] W. Xu, I. Cumming, A region-growing algorithm for insar phase unwrapping, Geoscience and Remote Sensing, IEEE Transactions on 37 (1) (1999) 124–134.

[8] A. Hooper, H. A. Zebker, Phase unwrapping in three dimensions with application to insar time series, J. Opt. Soc. Am. A 24 (9) (2007) 2737–2747.

[9] A. P. Shanker, H. Zebker, Edgelist phase unwrapping algorithm for time series insar analysis, J. Opt. Soc. Am. A 27 (3) (2010) 605–612.

[10] A. Pepe, L. Euillades, M. Manunta, R. Lanari, New advances of the extended minimum cost flow phase unwrapping algorithm for sbas-dinsar analysis at full spatial resolution, Geoscience and Remote Sensing, IEEE Transactions on 49 (10) (2011) 4062–4079.

[11] G. Fornaro, A. Pauciullo, D. Reale, A null-space method for the phase unwrapping of multitemporal sar interferometric stacks, Geoscience and Remote Sensing, IEEE Transactions on 49 (6) (2011) 2323–2334.

[12] M. Marghany, Three Dimensional Coastline Deformation from Insar Envisat Satellite Data, in: B. Murgante, S. Misra, M. Carlini, C. M. Torre, H.-Q. Nguyen, D. Taniar, B. O. Apduhan, O. Gervasi (Eds.), Computational Science and Its Applications -ICCSA 2013, Vol. 7972 of Lecture Notes in Computer Science, Springer Berlin Heidelberg, 2013, pp. 599–610.

[13] M. Marghany, DInSAR technique for three-dimensional coastal spit simulation from radarsat-1 fine mode data, Acta Geophysica 61 (2) (2013) 478–493.

[14] M. Marghany, Hybrid genetic algorithm of interferometric synthetic aperture radar for three-dimensional coastal deformation, Frontiers in Artificial Intelligence and Applications : New Trends in Software Methodologies, Tools and Technique 265 (2014) 116 – 131.

[15] T. Lan, D. Erdogmus, S. Hayflick, J. Szumowski, Phase unwrapping and background correction in MRI, in: Machine Learning for Signal Processing, 2008. MLSP 2008. IEEE Workshop on, 2008, pp. 239–243.

[16] K. Zhong, Z. Li, Y. Shi, C. Wang, Y. Lei, Fast phase measurement profilometry for arbitrary shape objects without phase unwrapping, Optics and Lasers in Engineering 51 (11) (2013) 1213 – 1222.

[17] T. Judge, P. Bryanston-Cross, A review of phase unwrapping techniques in fringe analysis, Optics and Lasers in Engineering 21 (4) (1994) 199 – 239.

[18] H. A. Zebker, Y. Lu, Phase unwrapping algorithms for radar interferometry: residue-cut, least-squares, and synthesis algorithms, J. Opt. Soc. Am. A 15 (3) (1998) 586–598.

[19] D. C. Ghiglia, M. D. Pritt, Two-Dimensional Phase Unwrapping: Theory, Algorithms, and Software, Wiley, 1998.

[20] M. Rivera, F. J. Hernandez-Lopez, A. Gonzalez, Phase unwrapping by accumulation of residual maps, Optics and Lasers in Engineering 64 (0) (2015) 51 – 58.

[21] D. L. Fried, Least-square fitting a wave-front distortion estimate to an array of phase-difference measurements, J. Opt. Soc. Am. 67 (3) (1977) 370–375.

[22] D. C. Ghiglia, L. A. Romero, Robust two-dimensional weighted and unweighted phase unwrapping that uses fast transforms and iterative methods, J. Opt. Soc. Am. A 11 (1) (1994) 107–117.

[23] M. Rivera, J. L. Marroquin, Half-quadratic cost functions for phase unwrapping, Optics Letters 29 (5) (2004) 504–506.

[24] D. C. Ghiglia, L. A. Romero, Minimum Lp-norm two-dimensional phase unwrapping, J. Opt. Soc. Am. A 13 (10) (1996) 1999–2013.

[25] E. de la Rosa-Miranda, E. Gonzalez-Ramirez, J. Villa-Hernandez, L. Berriel-Valdos, C. Olvera-Olvera, J. de la Rosa-Vargas, T. Saucedo-Anaya, J. A. Olague, D. Alaniz-Lumbreras, V. Castano, An alternative method for phase-unwrapping of interferometric data, Journal of the European Optical Society - Rapid publications 9 (0) (2014) 1–6.

[26] M. Black, P. Rangarajan, On the unification of line processes, outlier rejection, and robust statistics with applications in early vision, Int'l J. Computer Vision 19 (1) (1996) 57–91.